

Accepted Manuscript

Design, synthesis and molecular docking of salicylic acid derivatives containing metronidazole as a new class of antimicrobial agents

Zhi-Hua Guo, Yong Yin, Cong Wang, Peng-Fei Wang, Xing-Tao Zhang, Zhong-Chang Wang, Hai-Liang Zhu

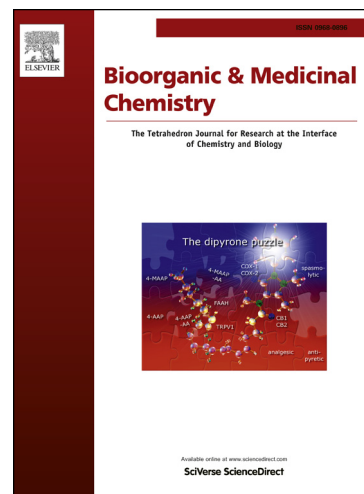
PII: S0968-0896(15)00659-8
DOI: <http://dx.doi.org/10.1016/j.bmc.2015.07.075>
Reference: BMC 12504

To appear in: *Bioorganic & Medicinal Chemistry*

Received Date: 20 June 2015
Revised Date: 30 July 2015
Accepted Date: 31 July 2015

Please cite this article as: Guo, Z-H., Yin, Y., Wang, C., Wang, P-F., Zhang, X-T., Wang, Z-C., Zhu, H-L., Design, synthesis and molecular docking of salicylic acid derivatives containing metronidazole as a new class of antimicrobial agents, *Bioorganic & Medicinal Chemistry* (2015), doi: <http://dx.doi.org/10.1016/j.bmc.2015.07.075>

This is a PDF file of an unedited manuscript that has been accepted for publication. As a service to our customers we are providing this early version of the manuscript. The manuscript will undergo copyediting, typesetting, and review of the resulting proof before it is published in its final form. Please note that during the production process errors may be discovered which could affect the content, and all legal disclaimers that apply to the journal pertain.



Design, synthesis and molecular docking of salicylic acid derivatives containing metronidazole as a new class of antimicrobial agents

Zhi-Hua Guo^{a, b}, Yong Yin^b, Cong Wang^a, Peng-Fei Wang^b, Xing-Tao Zhang^a,
Zhong-Chang Wang^{b*}, Hai-Liang Zhu^{b*}

^a*College of Biology and Food Engineering, SuZhou University, Suzhou, 234000,
People's Republic of China.*

^b*State Key Laboratory of Pharmaceutical Biotechnology, Nanjing University, Nanjing
210093, People's Republic of China.*

* *Corresponding author. Tel.: +86-25-83592572; Fax: +86-25-83592672.
E-mail address: zhuhl@nju.edu.cn (H.-L. Zhu).*

Abstract

A series of novel salicylic acid derivatives containing metronidazole as *S. aureus* Tyrosyl-tRNA synthetase (TyrRS) inhibitors have been synthesized and evaluated their biology activities as potential antibacterial agents. Among these compounds, compound **5r** exhibited the most potent antibacterial activity against Gram-positive (*S. aureus* ATCC 6538 and *B. subtilis* ATCC 6633) and Gram-negative (*E. coli* ATCC 35218 and *P. aeruginosa* ATCC 13525) with MICs of 0.39 ~ 1.57 $\mu\text{g}/\text{mL}$ and showed the most potent *S. aureus* Tyrosyl-tRNA synthetase inhibitory with 2.3 μM . Docking simulation was performed to insert compound **5r** into the crystal structure of *S. aureus* Tyrosyl-tRNA synthetase active site to determine the probable binding model. These results suggested that compound **5r** may be a promising antibacterial agent.

Keywords:

Salicylic acid derivatives

S. aureus TyrRS

Antibacterial activity

Molecular docking

1. Introduction

Bacterial infections are a serious threat to human health because of emerging resistance to existing antibiotics, so new antibacterial candidates will come from is an open problem.¹ In the past few decades the discovery of new antibacterial agents has proven very important challenging for the research community.² In order to resolve this serious puzzle, the crucial task of looking for new types of antibacterial agents should be achieved.³ So, much of the research are put into the design of new efficiency antibacterial agents against the challenge of the drug resistance.

New antibacterial agents which can work through different kinds of targets in key structures of the bacterial cells to overcome the problem of acquired resistance. Aminoacyl-tRNA synthetases (AARSs) is an enzyme which can recognize specific amino acids and ligate these amino acids to their cognate tRNA molecules during protein synthesis.⁴ When 1 of the 20 AARSs present in the cell is inhibited, the corresponding tRNA is not translated into protein, which leads to failure of protein synthesis and inhibition of cell growth.⁵ Because of these reasons, Aminoacyl-tRNA synthetases are essential for protein synthesis and cell viability. These enzymes are found in all living organisms, but there are great sequence differences between eukaryotes and prokaryotes.⁶ These properties suggest that small molecule inhibitors of AARSs could be promising drug candidates leading to high selectivity and broad-spectrum antibacterial agents.⁴ So, inhibitors of AARSs have been used as medicine or rigorously tested in clinical trials for therapeutic applications in microbial infections, such as, the natural product mupirocin, an inhibitor of Isoleucyl-tRNA synthetase (IleRS), is approved as a topical treatment for bacterial skin infections.⁷ Tyrosyl-tRNA synthetase (TyrRs) is one of the 20 Aminoacyl-tRNA synthetases and plays an important role in protein synthesis.⁸

Nitroimidazole derivatives have exhibited broad variety biological activities, particularly antibacterial activity.⁹ 5-Nitroimidazole based drugs have been extensively applied to cure the infections induced by bacteria and to kill pathogenic protozoan

parasites in human body.¹⁰⁻¹¹ So, nitroimidazole derivatives have attracted considerable attention of medicinal chemists as they can resist bio-reduction to generate electrophilic substances which can destroy proteins and acids.¹⁰ In the past decades, the toxicity and metabolism of nitroimidazole have been characterized, especially metronidazole.¹² In the past two years, we have already synthesized several compounds containing 5-nitroimidazole and evaluated for their antibacterial activities.^{6,13-16} In view of the above-mentioned findings, we continue to our previous study and designed, synthesized a novel series which have 5-nitroimidazole in skeleton as Tyrosyl-tRNA synthetase inhibitors, and which was evaluated for bacterial activity against Gram-positive (*S. aureus* ATCC 6538 and *B. subtilis* ATCC 6633) and Gram-negative (*E. coli* ATCC 35218 and *P. aeruginosa* ATCC 13525), and toxicity in human cells. At the beginning of the study, the molecular docking was performed to look for antibacterial target protein to determine who work with the designed compounds. The molecular docking of all the synthesized compounds and target proteins, such as FabH (PDB code: 1HNJ), DNA gyrase (PDB code: 3G75), Tyrosyl-tRNA synthetase (PDB code: 1JIJ) and Isoleucyl-tRNA synthetase (PDB code: 1JZQ), were performed by using the Discovery Studio 3.5. The results were presented in Fig. 1, it has been observed that the CDOCKER_INTERACTION_ENERGY between the designed compounds and protein 1JIJ is the lowest. The lower value of the CDOCKER_INTERACTION_ENERGY represented the potent binding affinity. This indicated that the designed compounds may have good inhibitory activity against Tyrosyl-tRNA synthetase.¹⁷⁻¹⁸ So we evaluated their antibacterial activities, and Tyrosyl-tRNA synthetase inhibitory activities.

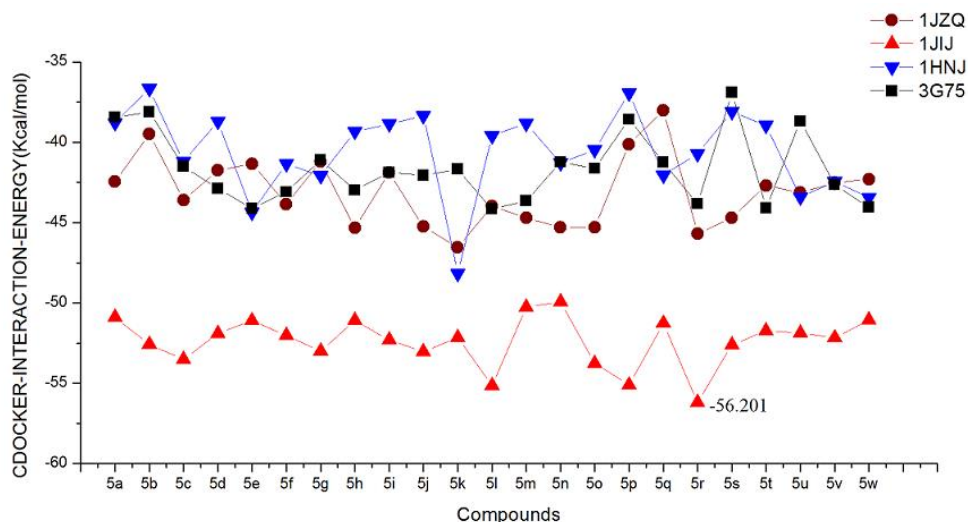


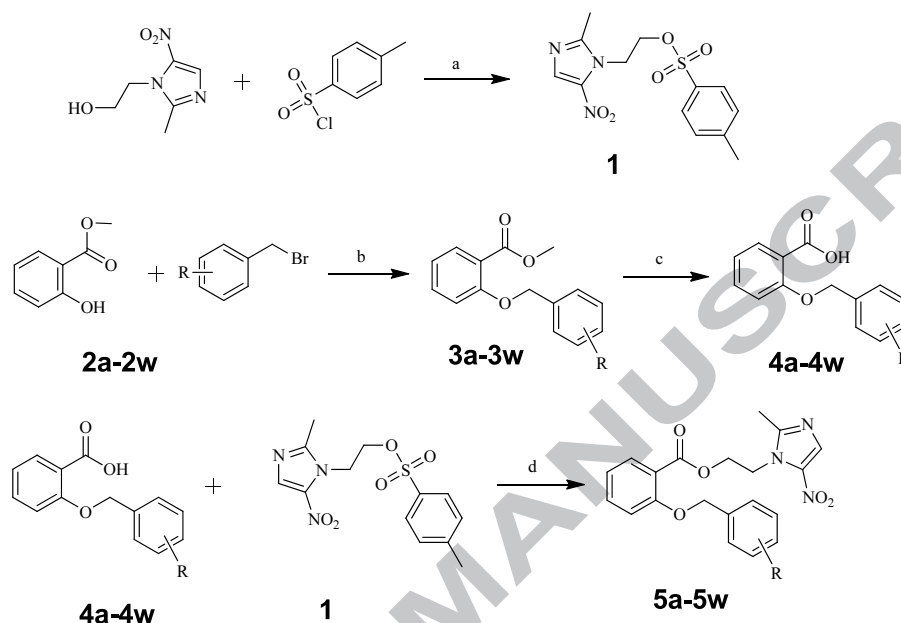
Fig. 1. The CDOCKER_INTERACTION_ENERGY (kcal/mol) obtained from the docking study of all synthesized compounds by the CDOCKER protocol (Discovery Studio 3.5, Accelrys, Co. Ltd).

2. Results and discussion

2.1 Chemistry

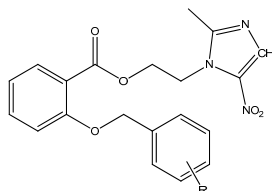
A series of novel salicylic acid derivatives were synthesized by the routes outlined in Scheme 1 and the structures of the desired compounds are shown in Table 1.¹⁹⁻²¹ The Met-OTs(2-(2-methyl-5-nitro-1H-imidazol-1-yl)-ethyl-4-methyl-benzenesulfonate, compound **1** was synthesized by the method in our previous paper.²¹ Firstly, compounds **3a-3w** were prepared by the reaction of methyl salicylate with different substituted benzyl bromide in acetone by adding potassium carbonate at 60 °C. Secondly, **3a-3w** were hydrolyzed using NaOH solution in EtOH which was heated at 60 °C for 6 h. After completion of the reaction, the solvent was evaporated, then 5M hydrochloric acid was slowly added to give a pH of 1~3 to get compounds **4a-4w**. Lastly, compounds **4a-4w** and Met-OTs were dissolved in DMF and refluxed to get the desired compounds **5a-5w**. The refined compounds **5a-5w** were finally obtained by subsequent purification with chromatography. All synthesized compounds were given satisfactory analytical and spectroscopic data which were in full accordance with their depicted

structures. Additionally, the structure of compound **5j** were determined by single crystal x-ray diffraction analysis in Table 2 and gave perspective views of compound **5j** with the atomic labeling system in Fig. 2. .



Scheme 1. The synthetic routes of compounds **5a-5w**. Reagents and conditions: (a) Et₃N, CH₂Cl₂, 0 °C, 6 h; (b) K₂CO₃, Me₂CO, 60°C, 6~8 h; (c) NaOH, EtOH, 60 °C, 6 h, pH 1~3; (d) K₂CO₃, DMF, 110 °C, 20~24 h.

Table 1. Structures of compounds **5a-5w**.



Compounds	R	Compounds	R
5a	H	5m	2-CF ₃
5b	2-F	5n	3-CF ₃
5c	3-F	5o	4-CF ₃
5d	4-F	5p	2, 6-F
5e	2-Cl	5q	3, 4-F
5f	3-Cl	5r	3, 4-Cl

5g	4-Cl	5s	2, 5-Cl
5h	4-Br	5t	3-F, 4-Cl
5i	4-CH ₃	5u	2-F, 3-Cl
5j	3, 5-CH ₃	5v	3,4,5-F
5k	4-CH(CH ₃) ₂	5w	2, 3, 4, 5, 6-F
5l	4-OCH ₃		

Table 2. Crystal structure data for compound **5j**.

Compound	5j
Formula	C ₂ H ₂₃ N ₃ O ₅
Mr	409.43
Crystal system	triclinic
Space group	<i>P</i> - 1
<i>a</i> / Å	7.2644(8)
<i>b</i> / Å	11.6040(12)
<i>c</i> / Å	12.4151(15)
α°	88.272(4)
β°	86.610(4)
γ°	83.315(2)
Volume / Å ³	1037.1(2)
<i>Z</i>	2
<i>D</i> <i>c</i> / (g/cm ³)	1.311
μ / mm ⁻¹	0.094
<i>F</i> (000)	432
Crystal size / mm ³	0.30×0.26×0.24
<i>T</i> / K	273(2)
θ Range / °	2.44/27.58
Index range (<i>h,k,l</i>)	-8/9, -14/13, -16/16
Reflections collected / unique	10652/4684[R(int)]=0.0315

Data/restraints/parameters	4684/0/274
Goodness-of-fit on F^2	1.065
R_1, wR_2 [$I > 2\sigma(I)$] ^A	0.0545/0.1281
R_1, wR_2 ^A	0.0930/0.1404
$(\Delta\rho)_{\max}, (\Delta\rho)_{\min}/(e/\text{\AA}^3)$	0.204/-0.289

ACCEPTED MANUSCRIPT

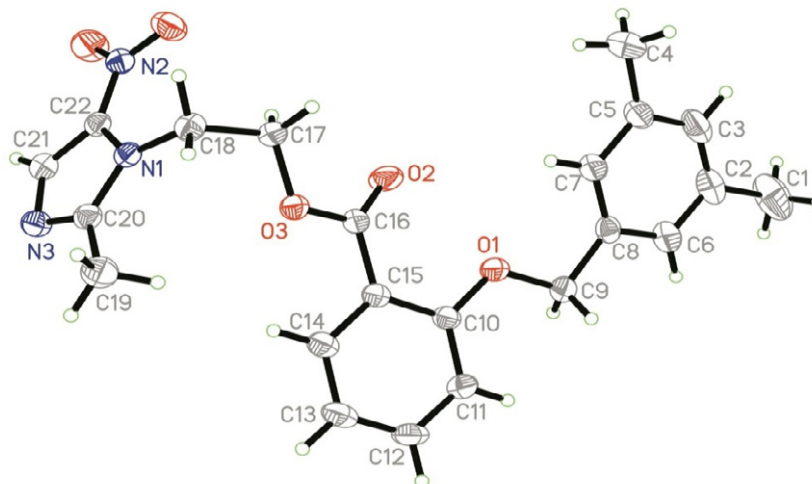


Fig. 2. Crystal structure diagram of compound 5j.

2.2 Biological activity

2.2.1 Antibacterial activity

The antibacterial efficacy of these compounds were evaluated against Gram-positive (*S. aureus* ATCC 6538 and *B. subtilis* ATCC 6633) and Gram-negative (*E. coli* ATCC 35218 and *P. aeruginosa* ATCC 13525) bacteria by the MH media dilution method. The MIC (minimum inhibitory concentration) values of these compounds were summarized in Table 3. Penicillin G and Chloramphenicol were also screened under identical conditions for comparison.

Table 3. Antibacterial activities of synthetic compounds.

Compounds	MIC ^a (µg/mL)			
	Gram-positive		Gram-negative	
	<i>B. subtilis</i> ATCC 6633	<i>S. aureus</i> ATCC 6538	<i>E. coli</i> ATCC 35218	<i>P. aeruginosa</i> ATCC 13525
5a	12.5	12.5	25	50
5b	25	12.5	50	50
5c	25	12.5	50	50
5d	12.5	12.5	25	25
5e	6.25	6.25	6.25	12.5
5f	6.25	6.25	12.5	12.5
5g	12.5	6.25	25	12.5

5h	6.25	6.25	12.5	12.5
5i	3.13	3.13	12.5	12.5
5j	1.57	3.13	6.25	12.5
5k	3.13	3.13	6.25	6.25
5l	0.78	1.57	6.25	6.25
5m	50	100	100	100
5n	100	50	100	100
5o	25	25	50	50
5p	25	25	50	50
5q	50	25	100	100
5r	0.78	0.39	3.13	1.57
5s	0.78	1.57	3.13	6.25
5t	3.13	3.13	6.25	6.25
5u	1.57	3.13	12.5	6.25
5v	25	25	100	50
5w	50	50	100	100
Penicillin G	0.78	0.78	6.25	6.25
Chloramphenicol	1.57	1.57	6.25	0.78

^a Values are the average of three independent experiments run in triplicate.

The results were shown in Table 3, the MICs differed greatly ranging from 0.39 ~ 100 $\mu\text{g}/\text{mL}$. Overall, most of the compounds exhibited better bacterial activities against Gram-positive bacteria strains than Gram-negative bacteria strains. Among them, compound **5r** displayed the most potent antibacterial activity, which had MIC values of 0.78, 0.39, 3.13 and 1.57 $\mu\text{g}/\text{mL}$ against *B. subtilis*, *S. aureus*, *P. aeruginosa* and *E. coli*, respectively, and was comparable to the antibiotic Penicillin G (corresponding MICs: 0.78, 0.78, 6.25 and 6.25 $\mu\text{g}/\text{mL}$) and chloramphenicol (corresponding MICs: 1.57, 1.57, 3.13 and 0.78 $\mu\text{g}/\text{mL}$).

The modification of substituents such as methoxyl, halogen, methyl was performed to explore the structure-activity relationships of these compounds. Compounds (**5g**, **5f**, **5e**, **5r**, **5s** and **5w**) with chlorine groups on benzyl ring exhibited antibacterial activities in the order of di-substituted > mono-substituted. Compounds **5r** and **5s**, which introduced

two chlorine atoms at 3, 4-position or 2, 5-position in benzene ring, showed that compounds with substitutes at 3, 4-position displayed better antibacterial activity than substitutes at 2, 5-position. Compared to **5r** and **5s**, compounds **5u** and **5t** showed more weak antibacterial activity. The MIC values of compound **5r** and **5s** (0.39 ~ 3.13 $\mu\text{g}/\text{mL}$ and 0.78 ~ 6.25 $\mu\text{g}/\text{mL}$), **5u** and **5t** (1.57 ~ 6.25 $\mu\text{g}/\text{mL}$ and 3.13 ~ 6.25 $\mu\text{g}/\text{mL}$) suggested that compounds with the same group of the benzene ring had more potent antibacterial activity than compounds with different groups. Interestingly, compounds (**5d**, **5p**, **5v** and **5w**) with fluoro groups on benzyl ring exhibited antibacterial activities in the order of mono-substituted > di-substituted > tri-substituted > multi-substituted, we concluded that the more electron withdrawing groups could reduce the electron density of the benzene ring and make it difficult to form π - π bonds with amino acids containing aromatic groups.²² This performance is particularly prominent in trifluoromethyl group, **5m** and **5n** showed worst antibacterial activity. Among compounds **5k**, **5i**, **5d**, **5g**, **5h**, **5o**, compounds with *para* substituted on phenyl ring exhibited antibacterial activities in order of electron-donating groups ($-\text{CH}_3$, $-\text{OCH}_3$ and $-\text{CH}(\text{CH}_3)_2$) > electron-withdrawing groups ($-\text{CF}_3$, $-\text{F}$, $-\text{Cl}$ and $-\text{Br}$). Among these compounds only one halogen atom at the 4-position of the phenyl ring, mostly, the strength order is $\text{Br} > \text{Cl} > \text{F}$.

Next, a comparison of the composition on the benzyl ring was displayed as follows: for compounds **5b-5d**, **5e-5g**, and **5m-5o**, the potency order was found as *para* > *ortho* > *meta* in substituent groups on benzyl ring. This indicated that the position of the substituent had an influence on the antibacterial activity.

2.2.2 *S. aureus* tyrosyl-tRNA inhibitory activity

In order to further study the mechanism by which the synthesized compounds induce antibacterial activity, the *S. aureus* Tyrosyl-tRNA inhibitory potency of the compounds were examined and summarized in Table 4. As we can see from Table 4, most of the tested compounds displayed potent Tyrosyl-tRNA inhibiting activity. Among them, compounds **5r**, displaying the most potent Tyrosyl-tRNA inhibitory activity with IC_{50}

of 2.3 μM . Compounds **5j**, **5s** and **5u** also displayed good inhibitory with IC_{50} of 3.0 μM , 2.7 μM and 2.9 μM . The results of *S. aureus* Tyrosyl-tRNA inhibitory activity of synthesized compounds (Table 4) were causally related to their antibacterial activity (Table 3). This indicated that antibacterial activity of the synthesized compounds would derived from the inhibition of Tyrosyl-tRNA enzymatic activities.

Table 4. Inhibitory effects of the synthetic compounds against *S. aureus* Tyrosyl-tRNA.

Compounds	<i>S.aureus</i> tyrosyl-tRNA	Hemolysis LC_{50}^a	Macrophage
	IC_{50} (μM)	(μM)	CC_{50}^b (μM)
5a	5.6 \pm 0.12	>10	231.2 \pm 1.13
5b	6.7 \pm 0.03	>10	154.7 \pm 2.32
5c	6.3 \pm 0.45	>10	123.6 \pm 2.33
5d	5.7 \pm 0.08	>10	156.9 \pm 1.78
5e	4.7 \pm 0.21	>10	213.3 \pm 1.22
5f	5.0 \pm 0.12	>10	187.7 \pm 1.78
5g	4.8 \pm 0.13	>10	167.5 \pm 1.98
5h	4.9 \pm 0.17	>10	198.5 \pm 1.74
5i	4.7 \pm 0.09	>10	139.8 \pm 1.28
5j	3.0 \pm 0.12	>10	251.7 \pm 0.76
5k	3.3 \pm 0.20	>10	271.8 \pm 0.56
5l	2.9 \pm 0.26	>10	238.7 \pm 0.98
5m	7.8 \pm 0.34	>10	233.0 \pm 1.69
5n	8.3 \pm 0.45	>10	250.6 \pm 2.64
5o	6.3 \pm 0.25	>10	241.7 \pm 2.46
5p	6.9 \pm 0.33	>10	276.8 \pm 1.76
5q	6.0 \pm 0.15	>10	256.4 \pm 1.24
5r	2.3 \pm 0.10	>10	187.7 \pm 1.15
5s	2.7 \pm 0.05	>10	193.4 \pm 1.27
5t	3.2 \pm 0.12	>10	179.7 \pm 1.78
5u	2.9 \pm 0.17	>10	190.5 \pm 2.61
5v	6.7 \pm 0.23	>10	267.4 \pm 2.30
5w	8.0 \pm 0.45	>10	236.4 \pm 1.80

^aLytic concentration 30%.

^b Minimum cytotoxic concentration required to cause a microscopically detectable alteration of normal cell morphology.

2.2.3 Cytotoxicity test

In order to find potent antibiotics, it is important to measure cytotoxicity. Good antibacterial agents not only have effective antibacterial activities, but also have no damage to mammalian cells that lead to high hemolytic and cytotoxic activity dangerous to the host organism. Generally, red blood cell is extremely fragile, hemolytic activity is used to measure the mammalian cell toxicity. Moreover, compounds were evaluated for their toxicity against human macrophage with the median cytotoxic concentration (CC₅₀) data by the MTT method.

So the hemolysis and cytotoxicity assays were both tested. The pharmacological results are showed in Table 4. As shown Table 4 tested compounds displayed low hemolytic activities and almost have no cytotoxicity activities in vitro against human macrophage. The cytotoxicity assay determined the selectivity of our compounds for bacteria over mammalian cells.

2.2.4 Drug-likeness analysis

Drug-like properties were calculated and the results were summarized in Table 5. Drug-like properties consist of molecular weight (MW), octanol–water partitioning coefficient (AlogP) based on Ghose and Crippen's method,²³ the number of hydrogen bond acceptors (HBA), the number of hydrogen bond donors (HBD) and molecular fractional polar surface area (MFPSA). All the data were calculated using the Discovery Studio molecular simulation package.²⁴ As shown in Table 5, all the desired compounds had AlogP value less than 5, MW less than 480 showed favorable values for the involved molecular parameters that is suitable for the Lipinski's Rule of Five.²⁵

Table 5. Molecular parameters of synthetic compounds.

Compounds	Molecular parameters				
	MW	AlogP ^a	HBA ^b	HBD ^c	MFPSA ^a
5a	381.382	3.273	4	0	0.267

5b	399.372	3.479	4	0	0.261
5c	399.372	3.479	4	0	0.261
5d	399.372	3.479	4	0	0.261
5e	415.827	3.938	4	0	0.251
5f	415.827	3.938	4	0	0.251
5g	415.827	3.938	4	0	0.251
5h	460.278	4.022	4	0	0.245
5i	395.409	3.76	4	0	0.254
5j	409.435	4.246	4	0	0.242
5k	423.462	4.468	4	0	0.234
5l	411.408	3.257	4	0	0.268
5m	449.38	4.216	4	0	0.241
5n	449.38	4.216	4	0	0.241
5o	449.38	4.216	4	0	0.241
5p	417.363	3.684	4	0	0.255
5q	417.363	3.684	4	0	0.255
5r	450.272	4.602	4	0	0.237
5s	450.272	4.602	4	0	0.237
5t	433.817	4.143	4	0	0.246
5u	433.817	4.143	4	0	0.246
5v	435.353	3.89	4	0	0.25
5w	471.334	4.301	4	0	0.24

^a Calculated by Discovery Studio 3.5.

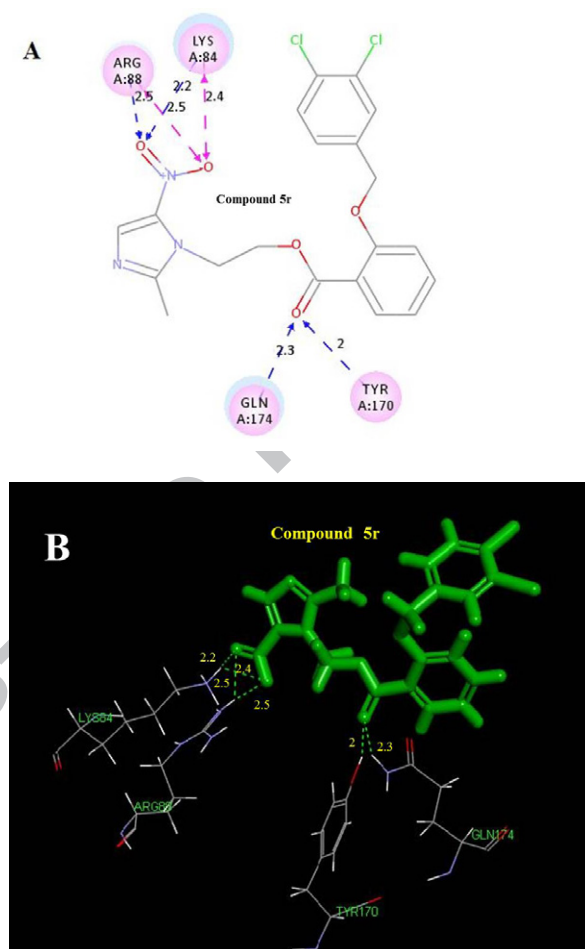
^b Counted as the sum of Ns and Os.

^c Counted as the sum of NHs and OHs.

2.2.5 Molecular docking

In order to study the interaction between binding model and bacterial activity, a docking study was performed to fit compound **5r** into the active center of the *S. aureus* Tyrosyl-tRNA (PDB:1JIJ). All docking runs were applied CDOCKER_DOCK protocol using Discovery Studio3.5. The binding model of compound **5r** with Tyrosyl-tRNA protein are presented in Fig. 3. . In the binding model, compound **5r** was well bound to the Tyrosyl-tRNA protein with Lys84, Arg88, Tyr170 and Gln174, the four amino acids located in the binding pocket of the protein played important action in the combination with compound **5r**. As we can see from Fig. 3. (A), Arg88 and Lys84 were respectively formed two charge interactions with oxygen atom of nitro group ($O\cdots H$: 2.5 Å and $O\cdots H$: 2.4 Å), which enhanced the combination activity of compound **5r**. Oxygen atom of nitro group formed two hydrogen bonds with the backbone NH of Arg88 ($N-O\cdots H$: 2.5 Å,

102.73°), Lys84 (N-O...H: 2.2 Å, 143.88°), respectively. And carboxyl oxygen formed two hydrogen bonds with Gln174 (C=O...H: 2.3 Å, 132.65°) and Tyr170 (C=O...H: 2.0 Å, 161.78°). The receptor surface model shown in Fig. 3. (C), which indicated that the compound **5r** was embedded into the Tyrosyl-tRNA protein active pocket. Docking results agreed with the antibacterial assay data, suggested that compound **5r** was a potential inhibitor of Tyrosyl-tRNA protein.



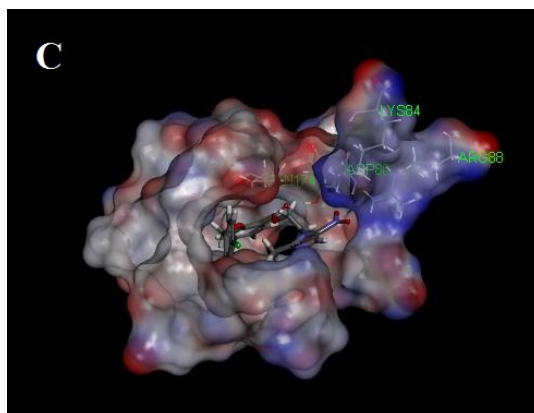


Fig. 3. Molecular docking modeling of compound **5r** with *S.aureus* Tyrosyl tRNA synthetase: or clarity, only interacting residues are displayed.

(A) 2D model of the interaction between compound **5r** and *S. aureus* Tyrosyl-tRNA synthetase. Blue dashed arrow represent the H-bond interactions with amino acids; pink dashed arrow represent the charge interactions.

(B) 3D model of the interaction between compound **5r** and *S. aureus* Tyrosyl-tRNA synthetase.

(C) The enzyme is shown as surface; while **5r** docked structures are shown as sticks.

3. Conclusion

In summary, a series of novel salicylic acid derivatives containing metronidazole had been designed and synthesized. These compounds were evaluated for their antibacterial activity against Gram-positive (*S. aureus* and *B. subtilis*) and Gram-negative (*E. coli* and *P. aeruginosa*). Out of these compounds, compound **5r** showed the most potent inhibitory activity against the tested bacteria strains with MICs of 0.39 ~ 3.13 $\mu\text{g}/\text{mL}$ and Tyrosyl-tRNA inhibitory activity with IC_{50} value of 2.3 μM . Molecular docking was performed to position compound **5r** into *S. aureus* Tyrosyl- tRNA active site to further determine the probable binding models and the result showed that compound **5r** was a potential Tyrosyl-tRNA inhibitor. This work might be useful for the design and synthesis of Tyrosyl-tRNA inhibitors with strong activities.

4. Experiments

4.1 Materials and measurements

All chemicals and reagents used in current study were analytical reagent or chemical pure. All reactions were routinely checked by thin-layer chromatography (TLC) on the glass-backed silica gel sheets (silica GF 254) and visualized using UV illumination. Flash column chromatography was performed on silica gel (200-300 mesh) eluting with ethyl acetate and petroleum ether. Melting points (uncorrected) were determined on a X-4 MP apparatus (Taikang Corp, Beijing, China). ^1H NMR spectra were recorded on a DPX 400 model spectrometer and reported in ppm using residual solvent as the internal standard (CDCl_3 at 7.24 ppm, $\text{DMSO}-d_6$ at 2.50 ppm). ESI-MS spectra were recorded on a Mariner System 5304 Mass Spectrometer. Elemental analyses were performed on a CHN-O-Rapid instrument and were within $\pm 0.4\%$ of the theoretical values. All the starting materials were commercially available unless otherwise indicated.

4.2 General method of synthesis of salicylic acid derivatives containing metronidazole

4.2.1 General synthetic procedure of Met-OTs (2-(2-methyl-5-nitro-1H-imidazol-1-yl) ethyl-4-methylbenzenesulfonate) (1)

All compounds described herein were synthesized by the following pathway depicted in Scheme 1. The key compound Met-OTs (2-(2-methyl-5-nitro-1H-imidazol-1-yl) ethyl-4-methylbenzenesulfonate), compound **1** has been synthesized from the metronidazole using the proper excess of tosyl chloride in the presence of trimethylamine in dichloromethane. Metronidazole (3.14 g, 20 mmol) and Et_3N (3.3 mL, 24 mmol) in CH_2Cl_2 (10 mL), and 4-methyl-benzenesulfonyl chloride (3.83 g, 20.1 mmol) in CH_2Cl_2 (10 mL) was added. The reaction mixture was stirred at $0\text{ }^\circ\text{C}$ for 6 h, then the mixture was evaporated under reduced pressure to afford a residue. The

residue was washed by petroleum ether for three times to remove remaining 4-methyl-benzenesulfonyl chloride. The product was dried to get a slight-yellow crystal of compound **1** (Met-OTs).

4.2.2 General synthetic procedure of methyl salicylate derivatives(**3a-3w**)

Compounds **3a-3w** were synthesized by the following procedure. Methyl salicylate (4 mmol), **2a-2w** (4 m mol) and K_2CO_3 (8 mmol) were added in acetone. The reaction was stirred at 60 °C for 6 ~ 8 h to gain **3a-3w**.

4.2.3 General synthetic procedure of salicylic acid derivatives(**4a-4w**)

3a-3w were hydrolyzed using 20% NaOH in EtOH which was stirred at 60 °C for 6 h. After reaction, the pH value of the solution was adjusted to 1 ~ 3 using 5M hydrochloric acid. The mixture was extracted with CH_2Cl_2 for three times. The organic layer was combined and dried with anhydrous Na_2SO_4 for 0.5 h to get **4a-4w**.

4.2.4 General synthetic procedure of salicylic acid derivatives containing metronidazole (**5a-5w**)

Met-OTs (2 mmol), **4a-4w** (2 mmol) and K_2CO_3 (4 mmol) were added in DMF (20 mL). The reaction was stirred at 110 °C for 20 ~ 24 h. The reaction mixture was poured into water and extracted with ethyl acetate (3×50 mL). The organic layer was combined and dried with anhydrous Na_2SO_4 for 0.5 h. Column chromatography was performed using silica gel (200 ~ 300 mesh) eluting with ethyl acetate and petroleum ether to obtain the desired compounds (**5a-5w**).

4.2.4.1. 2-(2-Methyl-5-nitro-1H-imidazol-1-yl)-ethyl-2-(benzyloxy)benzoate(**5a**).

Yellow solid, yield: 63.23%, mp: 78-80 °C. 1H NMR(400 MHz, $CDCl_3$) δ :2.43(s, 3H, CH_3), 4.68(s, 4H, CH_2), 5.19(s, 2H, CH_2), 7.02-7.07(m, 2H, ArH), 7.36-7.40(m, 1H, ArH), 7.42(s, 1H, ArH), 7.44(d, J=5.80 Hz, 2H, ArH), 7.47-7.48(m, 1H, ArH), 7.50-7.52(m, 1H, ArH), 7.73-7.75(m, 1H, ArH), 7.93(s, 1H, ArH). MS (ESI): 381.38

(C₂₀H₂₀N₃O₅, [M+H]⁺). Anal.Calcd for C₂₀H₁₉N₃O₅: C, 62.99; H, 5.02; N, 11.02%. Found: C, 63.12; H, 5.01; N, 11.04%.

4.2.4.2. 2-(2-Methyl-5-nitro-1H-imidazol-1-yl)-ethyl-2-((2-fluorobenzyl)-oxy)benzoate(5b).

Yellow solid, yield: 58.34%, mp: 89-91 °C. ¹H NMR(400 MHz, CDCl₃) δ : 2.46(s, 3H, CH₃), 4.69(s, 4H, CH₂), 5.25(s, 2H, CH₂), 7.03-7.14(m, 3H, ArH), 7.21(t, J=8.00 Hz, 1H, ArH), 7.32-7.38(m, 1H, ArH), 7.51-7.55(m, 1H, ArH), 7.59(t, J= 7.18 Hz, 1H, ArH), 7.73-7.75(m, 1H, ArH), 7.95 (s, 1H, ArH). MS (ESI): 399.37 (C₂₀H₁₉FN₃O₅, [M+H]⁺). Anal.Calcd for C₂₀H₁₈FN₃O₅: C, 60.15; H, 4.54; N, 10.52%. Found: C, 60.11; H, 4.55; N, 10.53%.

4.2.4.3. 2-(2-Methyl-5-nitro-1H-imidazol-1-yl)-ethyl-2-((3-fluorobenzyl)-oxy)benzoate(5c).

Yellow solid, yield: 59.07%, mp: 88-89 °C. ¹H NMR(400 MHz, CDCl₃) δ : 2.47(s, 3H, CH₃), 4.72(s, 4H, CH₂), 5.19(s, 2H, CH₂), 7.02-7.08(m, 3H, ArH), 7.23(t, J=6.34 Hz, 2H, ArH), 7.39(m, 1H, ArH), 7.50-7.54(m, 1H, ArH), 7.76(d, J=7.72 Hz, 1H, ArH), 7.94(s, 1H, ArH). MS (ESI): 399.37 (C₂₀H₁₉FN₃O₅, [M+H]⁺). Anal.Calcd for C₂₀H₁₈FN₃O₅: C, 60.15; H, 4.54; N, 10.52%. Found: C, 60.05; H, 4.52; N, 10.53%

4.2.4.4. 2-(2-Methyl-5-nitro-1H-imidazol-1-yl)-ethyl-2-((4-fluorobenzyl)-oxy)benzoate(5d).

Yellow solid, yield: 62.18%, mp: 90-92 °C. ¹H NMR(400 MHz, CDCl₃) δ : 2.46(s, 3H, CH₃), 4.70(s, 4H, CH₂), 5.14(s, 2H, CH₂), 7.01-7.07(m, 2H, ArH), 7.35(d, J=8.16 Hz, 2H, ArH), 7.49-7.56(m, 3H, ArH), 7.73(d, J=7.72 Hz, 1H, ArH), 7.95(s, 1H, ArH). MS (ESI): 399.37(C₂₀H₁₉FN₃O₅, [M+H]⁺). Anal.Calcd for C₂₀H₁₈FN₃O₅: C, 60.15; H, 4.54; N, 10.52%. Found: C, 60.05; H, 4.55; N, 10.54%.

4.2.4.5. 2-(2-Methyl-5-nitro-1H-imidazol-1-yl)-ethyl-2-((2-chlorobenzyl)-oxy)benzoate(5e).

oate(5e).

Yellow solid, yield: 68%, mp: 99-101 °C. ¹H NMR(400 MHz, CDCl₃) δ : 2.46(s, 3H, CH₃), 4.69(s, 4H, CH₂), 5.25(s, 2H, CH₂), 7.02-7.08(m, 2H, ArH), 7.29(t, *J*=6.92 Hz, 1H, ArH), 7.34(t, *J*=8.00 Hz, 1H, ArH), 7.41(d, *J*=7.46 Hz, 1H, ArH), 7.52(t, *J*=7.88 Hz, 1H, ArH), 7.68(d, *J*=7.52 Hz, 1H, ArH), 7.75(d, *J*=8.00 Hz, 1H, ArH), 7.94(s, 1H, ArH). MS (ESI): 415.83 (C₂₀H₁₉ClN₃O₅, [M+H]⁺). Anal.Calcd for C₂₀H₁₈ClN₃O₅: C, 57.77; H, 4.36; N, 10.11%. Found: C, 57.79; H, 4.34; N, 10.18%.

4.2.4.6. 2-(2-Methyl-5-nitro-1H-imidazol-1-yl)-ethyl-2-((3-chlorobenzyl)-oxy)benzoate(5f).

Yellow solid, yield: 76.27%, mp: 90-91 °C. ¹H NMR(400 MHz, CDCl₃) δ : 2.46(s, 3H, CH₃), 4.72(s, 4H, CH₂), 5.16(s, 2H, CH₂), 7.01-7.08(m, 2H, ArH), 7.33(d, *J*=14.68 Hz, 3H, ArH), 7.52(t, *J*=9.08 Hz, 2H, ArH), 7.76(d, *J*=5.60 Hz, 1H, ArH), 7.93(s, 1H, ArH). MS (ESI): 415.83 (C₂₀H₁₉ClN₃O₅, [M+H]⁺). Anal.Calcd for C₂₀H₁₈ClN₃O₅: C, 57.77; H, 4.36; N, 10.11%. Found: C, 57.79; H, 4.32; N, 10.09%.

4.2.4.7. 2-(2-Methyl-5-nitro-1H-imidazol-1-yl)-ethyl-2-((4-chlorobenzyl)-oxy)benzoate(5g).

Yellow solid, yield: 76.87%, mp: 91-93 °C. ¹H NMR(400 MHz, CDCl₃) δ : 2.48(s, 3H, CH₃), 4.72(s, 4H, CH₂), 5.15(s, 2H, CH₂), 7.00(d, *J*=8.36 Hz, 1H, ArH), 7.04-7.08(m, 1H, ArH), 7.19-7.21(m, 1H, ArH), 7.31(s, 1H, ArH), 7.44(t, *J*=7.84 Hz, 1H, ArH), 7.50-7.54(m, 2H, ArH), 7.74-7.76(m, 1H, ArH), 7.96(s, 1H, ArH). MS (ESI): 415.83 (C₂₀H₁₉ClN₃O₅, [M+H]⁺). Anal.Calcd for C₂₀H₁₈ClN₃O₅: C, 57.77; H, 4.36; N, 10.11%. Found: C, 57.80; H, 4.41; N, 10.16%.

4.2.4.8. 2-(2-Methyl-5-nitro-1H-imidazol-1-yl)-ethyl-2-((4-bromobenzyl)-oxy)benzoate(5h).

Yellow solid, yield: 74.26%, mp: 109-110 °C. ¹H NMR(400 MHz, CDCl₃) δ : 2.46(s,

3H, CH₃), 4.70(s, 4H, CH₂), 5.1(s, 2H, CH₂), 7.01-7.06(m, 2H, ArH), 7.35(d, *J*=8.16 Hz, 2H, ArH), 7.49-7.56(m, 3H, ArH), 7.73(d, *J*=7.72 Hz, 1H, ArH), 7.95(s, 1H, ArH). MS (ESI): 460.28 (C₂₀H₁₉BrN₃O₅, [M+H]⁺). Anal.Calcd for C₂₀H₁₈BrN₃O₅: C, 52.19; H, 3.94; N, 9.13%. Found: C, 52.25; H, 3.99; N, 9.21%.

4.2.4.9. 2-(2-Methyl-5-nitro-1H-imidazol-1-yl)-ethyl-2-((4-methylbenzyl)-oxy)benzoate(5i).

Yellow crystal, yield: 77.16%, mp: 98-99 °C. ¹H NMR(400 MHz, CDCl₃) δ : 2.40(s, 3H, CH₃), 2.43(s, 3H, CH₃), 4.67(s, 4H, CH₂), 5.14(s, 2H, CH₂), 7.00-7.06(m, 2H, ArH), 7.22(d, *J*=7.8 Hz, 2H, ArH), 7.33(d, *J*=7.84 Hz, 2H, ArH), 7.50(t, *J*=7.88 Hz, 1H, ArH), 7.73(d, *J*=7.68 Hz, 1H, ArH), 7.93(s, 1H, ArH). MS (ESI): 395.41 (C₂₁H₂₂N₃O₅, [M+H]⁺). Anal.Calcd for C₂₀H₂₁N₃O₅: C, 63.92; H, 5.35; N, 10.63%. Found: C, 63.79; H, 5.33; N, 10.63%.

4.2.4.10. 2-(2-Methyl-5-nitro-1H-imidazol-1-yl)-ethyl-2-((3, 5-dimethylbenzyl)-oxy)benzoate(5j).

Yellow crystal, yield: 76.18%, mp: 96-97 °C. ¹H NMR(400 MHz, CDCl₃) δ : 2.36(s, 6H, CH₃), 2.44(s, 3H, CH₃), 4.68-4.69(m, 4H, CH₂), 5.12(s, 2H, CH₂), 6.99-7.07(m, 5H, ArH), 7.47-7.52(m, 1H, ArH), 7.72-7.74(m, 1H, ArH), 7.94(s, 1H, ArH). MS (ESI): 409.16 (C₂₂H₂₄N₃O₅, [M+H]⁺). Anal.Calcd for C₂₀ C₂₂H₂₃N₃O₅: C, 64.54; H, 5.66; N, 10.26%. Found: C, 64.70; H, 5.68; N, 10.29%.

4.2.4.11. 2-(2-Methyl-5-nitro-1H-imidazol-1-yl)-ethyl-2-((4-isopropylbenzyl)-oxy)benzoate(5k).

Yellow solid, yield: 67.54%, mp: 80-81 °C. ¹H NMR(400 MHz, CDCl₃) δ : 1.28-1.31 (d, *J*=6.92 Hz, 6H, CH₃), 2.43(s, 3H, CH₃), 2.93-2.99(m, 1H, CH), 4.67(s, 4H, CH₂), 5.15(s, 2H, CH₂), 7.02(t, *J*=7.50 Hz, 1H, ArH), 7.07(d, *J*=8.40 Hz, 1H, ArH), 7.29(t, *J*=7.90 Hz, 1H, ArH), 7.38(d, *J*=7.92 Hz, 2H, ArH), 7.50(t, *J*=7.84 Hz, 1H, ArH), 7.72 (d, *J*=7.64 Hz, 1H, ArH), 7.94(s, 1H, ArH). MS (ESI): 423.46 (C₂₃H₂₆N₃O₅, [M+H]⁺). Anal.Calcd for C₂₃H₂₅N₃O₅: C, 65.24; H, 5.95; N, 9.92%. Found: C, 65.09; H, 5.93; N,

9.89%.

4.2.4.12. 2-(2-Methyl-5-nitro-1H-imidazol-1-yl)-ethyl-2-((4-methoxybenzyl)-oxy)benzoate(5l).

Yellow solid, yield: 63.94%, mp: 85-86 °C. ¹H NMR(400 MHz, CDCl₃) δ : 2.40(s, 3H, CH₃), 2.47(s, 3H, CH₃), 4.67(s, 4H, CH₂), 5.14(s, 2H, CH₂), 7.00-7.06(m, 2H, ArH), 7.22(d, *J*=7.8 Hz, 2H, ArH), 7.33(d, *J*=7.84 Hz, 2H, ArH), 7.50(t, *J*=7.88 Hz, 1H, ArH), 7.73(d, *J*=7.68 Hz, 1H, ArH), 7.93(s, 1H, ArH). MS (ESI): 411.41 (C₂₁H₂₂N₃O₆, [M+H]⁺). Anal.Calcd for C₂₁H₂₁N₃O₆: C, 61.31; H, 5.14; N, 10.21%. Found: C, 61.48; H, 5.15; N, 10.23%.

4.2.4.13. 2-(2-Methyl-5-nitro-1H-imidazol-1-yl)-ethyl-2-((2-(trifluoromethyl)-benzyl)-oxy)benzoate(5m).

Yellow solid, yield: 58.48%, mp: 92-93 °C. ¹H NMR(400 MHz, CDCl₃) δ : 2.48(s, 3H, CH₃), 4.72(s, 4H, CH₂), 5.39(s, 2H, CH₂), 7.04-7.07(m, 2H, ArH), 7.45-7.55(m, 2H, ArH), 7.64(t, *J*=7.61 Hz, 1H, ArH), 7.73(d, *J*=7.84 Hz, 1H, ArH), 7.77(d, *J*=7.68 Hz, 1H, ArH), 7.93(d, *J*=7.88 Hz, 1H, ArH), 7.96(s, 1H, ArH). MS (ESI): 449.38 (C₂₁H₁₉F₃N₃O₅, [M+H]⁺). Anal.Calcd for C₂₁H₁₈F₃N₃O₅: C, 56.13; H, 4.04; N, 9.35%. Found: C, 56.26; H, 4.03; N, 9.37%.

4.2.4.14. 2-(2-Methyl-5-nitro-1H-imidazol-1-yl)-ethyl-2-((3-(trifluoromethyl)-benzyl)-oxy)benzoate(5n).

Yellow solid, yield: 68.31%, mp: 78-80 °C. ¹H NMR(400 MHz, CDCl₃) δ : 2.46(s, 3H, CH₃), 4.71(s, 4H, CH₂), 5.24(s, 2H, CH₂), 7.04-7.09(m, 2H, ArH), 7.53(t, *J*=9 Hz, 1H, ArH), 7.57(d, *J*=7.84 Hz, 1H, ArH), 7.64(d, *J*=7.64 Hz, 1H, ArH), 7.68(d, *J*=7.52 Hz, 1H, ArH), 7.78(m, 2H, ArH), 7.91(s, 1H, ArH). MS (ESI): 449.38 (C₂₁H₁₉F₃N₃O₅, [M+H]⁺). Anal.Calcd for C₂₁H₁₈F₃N₃O₅: C, 56.13; H, 4.04; N, 9.35%. Found: C, 56.28; H, 4.05; N, 9.39%.

4.2.4.15. 2-(2-Methyl-5-nitro-1H-imidazol-1-yl)-ethyl-2-((4-(trifluoromethyl)-benzyl)-oxy)benzoate(5o).

Yellow crystal, yield: 73.03%, mp: 148-149 °C. ¹H NMR(400 MHz, CDCl₃) δ : 2.47(s,

3H, CH₃), 4.71(s, 4H, CH₂), 5.24(s, 2H, CH₂), 7.01-7.08(m, 2H, ArH), 7.50-7.54(m, 1H, ArH), 7.61(d, *J*=8.08 Hz, 2H, ArH), 7.69(d, *J*=7.52 Hz, 2H, ArH), 7.74-7.76(m, 1H, ArH), 7.94(s, 1H, ArH). MS (ESI): 449.38 (C₂₁H₁₉F₃N₃O₅, [M+H]⁺). Anal.Calcd for C₂₁H₁₈F₃N₃O₅: C, 56.13; H, 4.04; N, 9.35%. Found: C, 56.23; H, 4.03; N, 9.41%.

4.2.4.16. 2-(2-Methyl-5-nitro-1H-imidazol-1-yl)-ethyl-2-((2, 6-difluorobenzyl)-oxy) benzoate(5p).

Yellow solid, yield: 69.06%, mp: 113-114 °C. ¹H NMR(400 MHz, CDCl₃) δ : 2.44(s, 3H, CH₃), 4.62(s, 4H, CH₂), 5.22(s, 2H, CH₂), 6.94-6.98(t, *J*=7.84 Hz, 2H, ArH), 7.07(t, *J*=7.52 Hz, 2H, ArH), 7.20(d, *J*=8.36 Hz, 1H, ArH), 7.34-7.41(m, 1H, ArH), 7.53-7.57(m, 1H, ArH), 7.69(t, *J*=7.72 Hz, 2H, ArH), 7.98(s, 1H, ArH). MS (ESI): 417.36(C₂₀H₁₈F₂N₃O₅, [M+H]⁺). Anal.Calcd for C₂₀H₁₇F₂N₃O₅: C, 57.56; H, 4.11; N, 10.07%. Found: C, 57.63; H, 4.18; N, 10.17%

4.2.4.17. 2-(2-Methyl-5-nitro-1H-imidazol-1-yl)-ethyl-2-((3, 4-difluorobenzyl)-oxy) benzoate(5q).

Yellow solid, yield: 71.85%, mp: 105-106 °C. ¹H NMR(400 MHz, CDCl₃) δ : 2.48(s, 3H, CH₃), 4.70-4.73(m, 4H, CH₂), 5.13(s, 2H, CH₂), 7.00-7.06(m, 1H, ArH), 7.19-7.23(m, 1H, ArH), 7.31-7.37(m, 1H, ArH), 7.52-7.54(m, 1H, ArH), 7.73-7.76(m, 1H, ArH), 7.95(s, 1H, ArH). MS (ESI): 417.36(C₂₀H₁₈F₂N₃O₅, [M+H]⁺). Anal.Calcd for C₂₀H₁₇F₂N₃O₅: C, 57.56; H, 4.11; N, 10.07%. Found: C, 57.61; H, 4.09; N, 10.08%.

4.2.4.18. 2-(2-Methyl-5-nitro-1H-imidazol-1-yl)-ethyl-2-((3, 4-dichlorobenzyl)-oxy) benzoate(5r).

Yellow solid, yield: 77.27%, mp: 143-144 °C. ¹H NMR(DMSO-*d*₆, 400 MHz) δ : 2.40(s, 3H, CH₃), 4.62(t, *J*=4.78 Hz, 2H, CH₂), 4.69(t, *J*=4.82 Hz, 2H, CH₂), 5.20(s, 2H, CH₂), 7.06(t, *J*=7.52 Hz, 1H, ArH), 7.21(d, *J*=8.4 Hz, 1H, ArH), 7.40-7.42(m, 1H, ArH), 7.54-7.59(m, 1H, ArH), 7.61-7.63(m, 1H, ArH), 7.65(d, *J*=8.28 Hz, 1H, ArH), 7.71(s, 1H, ArH), 7.98(s, 1H, ArH). MS (ESI): 450.27 (C₂₀H₁₈Cl₂N₃O₅, [M+H]⁺). Anal.Calcd for C₂₀H₁₇Cl₂N₃O₅: C, 53.35; H, 3.81; N, 9.33%. Found: C, 53.29; H, 3.85; N, 9.39%.

4.2.4.19. 2-(2-Methyl-5-nitro-1H-imidazol-1-yl)-ethyl-2-((2, 6-dichlorobenzyl)-oxy)

benzoate(5s).

Yellow solid, yield: 76.16%, mp: 109-110 °C. ¹H NMR(400 MHz, CDCl₃) δ : 2.47(s, 3H, CH₃), 4.76(s, 4H, CH₂), 5.20(s, 2H, CH₂), 7.08(t, J=7.58 Hz, 2H, ArH), 7.27-7.29(m, 1H, ArH), 7.36(d, J=8.48 Hz, 1H, ArH), 7.54-7.58(m, 1H, ArH), 7.77-7.82(m, 2H, ArH), 7.94(s, 1H, ArH). MS (ESI): 450.27(C₂₀H₁₈Cl₂N₃O₅, [M+H]⁺). Anal.Calcd for C₂₀H₁₇Cl₂N₃O₅: C, 53.35; H, 3.81; N, 9.33%. Found: C, 53.30; H, 3.88; N, 9.41%.

4.2.4.20. 2-(2-Methyl-5-nitro-1H-imidazol-1-yl)-ethyl-2-((4-chloro-3-fluorobenzyl)-oxy)benzoate(5t).

Yellow solid, yield:74.28%, mp: 121-122 °C. ¹H NMR(400 MHz, CDCl₃) δ : 2.48(s, 3H, CH₃), 4.72(s, 4H, CH₂), 5.15(s, 2H, CH₂), 6.99-7.01(d, J=8.36 Hz, 1H, ArH), 7.04-7.08(m, 1H, ArH), 7.19-7.21(m, 1H, ArH), 7.31(s, 1H, ArH), 7.43(t, J=7.84 Hz, 1H, ArH), 7.50-7.54(m, 1H, ArH), 7.74-7.76(m, 1H, ArH), 7.96(s, 1H, ArH). MS (ESI): 433.82 (C₂₀H₁₈ClFN₃O₅, [M+H]⁺). Anal.Calcd for C₂₀H₁₇ClFN₃O₅: C, 55.37; H, 3.95; N, 9.69%. Found: C, 55.42; H, 4.00; N, 9.76%.

4.2.4.21. 2-(2-Methyl-5-nitro-1H-imidazol-1-yl)-ethyl-2-((3-chloro-2-fluorobenzyl)-oxy)benzoate(5u).

Yellow solid, yield: 58.15%, mp: 113-114 °C. ¹H NMR(400 MHz, CDCl₃) δ : 2.51(s, 3H, CH₃), 4.69-4.74(s, 4H, CH₂), 5.26(s, 2H, CH₂), 7.06-7.10(m, 2H, ArH), 7.15-7.19(m, 1H, ArH), 7.40-7.44(m, 1H, ArH), 7.51-7.58(m, 2H, ArH), 7.74-7.76(m, 1H, ArH), 7.97(s, 1H, ArH). MS (ESI): 433.82 (C₂₀H₁₈ClFN₃O₅, [M+H]⁺). Anal.Calcd for C₂₀H₁₇ClFN₃O₅: C, 55.37; H, 3.95; N, 9.69%. Found: C, 55.42; H, 3.99; N, 9.73%.

4.2.4.22. 2-(2-Methyl-5-nitro-1H-imidazol-1-yl)-ethyl-2-((3, 4, 5-trifluorobenzyl)-oxy)benzoate(5v).

Yellow solid, yield: 57.74%, mp: 148-149 °C. ¹H NMR(400 MHz, CDCl₃) δ : 2.52(s, 3H, CH₃), 4.72-4.78(m, 4H, CH₂), 5.12(s, 2H, CH₂), 6.99(d, J=8.32 Hz, 1H, ArH), 7.06-7.10(m, 1H, ArH), 7.16(t, J=7.3 Hz, 2H, ArH), 7.52-7.56(m, 1H, ArH), 7.75-7.78(m, 1H, ArH), 7.97(s, 1H, ArH). MS (ESI): 435.35 (C₂₀H₁₇F₃N₃O₅, [M+H]⁺). Anal.Calcd for C₂₀H₁₆F₃N₃O₅: C, 55.18; H, 3.70; N, 9.65%. Found: C, 55.08; H, 3.78;

N, 9.73%.

4.2.4.23. 2-(2-Methyl-5-nitro-1H-imidazol-1-yl)-ethyl-2-((perfluorophenyl)-methoxy)benzoate(5w).

Yellow solid, yield: 57.79%, mp: 166-167 °C. ¹H NMR(400 MHz, CDCl₃) δ : 2.47(s, 3H, CH₃), 4.64-4.70(m, 4H, CH₂), 5.25(s, 2H, CH₂), 7.08-7.18(m, 2H, ArH), 7.55(t, *J*=7.82 Hz, 1H, ArH), 7.70(d, *J*=7.68 Hz, 1H, ArH), 7.98(s, 1H, ArH). MS (ESI): 471.33 (C₂₀H₁₅F₅N₃O₅, [M+H]⁺). Anal.Calcd for C₂₀H₁₄F₅N₃O₅: C, 50.96; H, 2.99; N, 8.92%. Found: C, 50.88; H, 2.91; N, 8.99%.

4.3. Crystal structure determination

Compound **5j** of X-ray single-crystal diffraction data was collected on a Bruker D-8 venture diffractometer equipped with graphite monochromated Mo K α (λ = 0.71073 Å) radiation by the ω scan mode. Structure solution, refinement and data output were carried out with the SHELXTL-NT program package.²⁶ All the non-hydrogen atoms were refined anisotropically. All the hydrogen atoms were placed in calculated positions and were assigned fixed isotropic thermal parameters at 1.2 times the equivalent isotropic U of the atoms to which they are attached and allowed to ride on their respective parent atoms. The contributions of these hydrogen atoms were included in the structure-factors calculations. The crystal data, data collection and refinement parameters for the compound **5j** were listed in Table 2.

4.4. In Vitro Antimicrobial Activity Experiments

The minimum inhibitory concentration (MIC) was tested against two Gram-positive bacterial strains (*B. subtilis* ATCC 6633 and *S. aureus* ATCC 6538) and two Gram-negative bacterial strains (*E. coli* ATCC 35218 and *P. aeruginosa* ATCC 13525).²⁷ The MIC values were determined using the broth microdilution method according to the standards Institute (CLSI) as previously described.²⁸ Synthesized compounds were dissolved in 50% water in DMSO to prepare a stock solution that had a concentration of 0.5 mg/mL. Serial 2-fold dilutions were prepared from the stock solution with MH media and poured into 96-well plates. The tested bacteria were

grown in MH media at 37 °C for 24 h and were justed to the turbidity of the 0.5 McFarland standard. These bacterial suspensions were added to 96-well plates to obtain the compound concentrations of 25, 12.5, 6.25, 3.13, 1.57, 0.79 µg/mL and even lower concentrations. An inoculated micro-dilution trays were incubated in ambient air at 37 °C for 18 h. The MIC values were recorded as the lowest concentration of compounds showing no growth of bacteria.²⁹ MIC values were determined at least twice on separate days, with the higher value used to represent the MIC value. Penicillin G and chloramphenicol were used as standards for bacteria. The observed MICs were presented in Table 3.

4.5. *S. aureus* TyrRS inhibitory activity

S. aureus TyrRS was over-expressed in *E. coli* BL21 and purified to near homogeneity using standard purification procedures.³⁰ TyrRS activity was measured by aminoacylation using modifications to previously described methods.⁸ The assays were performed at 37 °C in a mixture containing (final concentrations) 100 mM Tris-HCl pH 8.0, 50 mM KCl, 16 mM MgCl₂, 5 mM ATP, 3 mM DTT, 4 mg/mL MRE600 tRNA (Roche) and 10 µM L-tyrosine (0.3 mM L-[ring-3,5-³H] tyrosine (PerkinElmer, Specific activity: 1.48-2.22 TBq/mmol), 10 µM carrier). TyrRS (0.2 nM) was pre-incubated with a range of inhibitor concentrations 25, 12.5, 6.25 3.13, 1.56 and 0.78 µM for 10 min at room temperature followed by the addition of pre-warmed mixture at 37 °C." After specific intervals, the reaction was terminated by adding aliquots of the reaction mixture into ice-cold 7% trichloroacetic acid and harvesting onto 0.45 µm hydrophilic Durapore filters (Millipore Multiscreen 96-well plates) and counted by liquid scintillation. The rate of reaction in the experiments was linear with respect to protein and time with less than 50% total tRNA acylation. IC₅₀ values corresponding to the concentration at which half of the enzyme activity is inhibited by the compound. The results were showed in Table 4.

4.6. Hemolysis test

Hemolytic activity was assayed using fresh capillary human blood. Erythrocytes were collected by centrifuging the blood three times in chilled phosphate buffered saline (PBS at 4 °C) at 1000 g for 10 min. The final pellet was resuspended in PBS to give a 2% w/v solution. Using a microtiter plate, 100 μ L of the erythrocyte solution was added to dextran, PLL, stearyl-PLL or stearyl-PLL+ LDL (1–1000 μ g/mL) in a volume of 100 μ L. Samples were then incubated for 3 h and the microtiter plate was then centrifuged at 1000 g for 10 min and the supernatants (100 μ L) transferred into a new microtiter plate. Hemoglobin release was determined spectrophotometrically using a microtiter plate reader (absorbance at 550 nm). Results were expressed as the amount of released hemoglobin induced by the compounds as a percentage of the total.

4.7. Cytotoxicity test

The cytotoxic activity in vitro was measured against mammalian cells, human macrophage using the MTT assay. The cell was grown in DMEM medium supplemented with 10% FBS and 1 \times antimycotic and antibacterial solution (sigma USA) at 37 °C, in humidified atmosphere having 5% CO₂. 100 μ L of the confluent fibroblast stock suspension was dispensed in 96-well tissue culture plate. The original medium from the wells was replaced with 100 μ L serum free DMEM when the cells reached 90% confluence after 5 h incubation in a CO₂ incubator. Various concentrations of the compounds were added to the growing cells and incubated for 24 h. The absorbance was measured at a wavelength of 570 nm on an ELISA microplate reader. Three replicate wells were used for each concentration and each assay was measured three times, after which the average of IC₅₀ was calculated. The cytotoxicity of each compound was expressed as the concentration of compound that reduced cell viability to 50% (IC₅₀). The results were summarized in Table 4.

4.8. Docking simulations

The crystal structure of *S. aureus* Tyrosyl-tRNA synthetase (PDB code: 1JII) was obtained from the Protein Data Bank (<http://www.rcsb.org>). Molecular docking of compound **5r** into the three-dimensional X-ray structure of Tyrosyl-tRNA synthetase was carried out using CDOCKER_DOCK protocol of Discovery Studio 3.5.

Acknowledgment

This work was supported by Science Research Project of Education Department of Anhui Province (KJ2013B286).

References and notes

1. Fischbach, M. A.; Walsh, C. T. *Science*. **2009**, 325, 1089.
2. Botella, G. M.; Breen, J. N.; Duffy, J. E. S.; Dumas, J.; Geng, B.; Gowers, I. K.; Green, O. M.; Guler, S.; Hentemann, M. F.; Juan, F. A. *J. Med. Chem.* **2012**, 55, 10010.
3. Lee, M. *Nature*. **2004**, 431, 892.
4. Kim, S.; Lee, S. W.; Choi, E.C.; Choi, S. Y. *Appl. Microbiol. Biot.* **2003**, 61, 278.
5. Vijver, P. V.; Vondenhoff, G. H.; Kazakov, T. S.; Semenova, E.; Kuznedelov, K.; Metlitskaya, A.; Aerschot, A.V.; Severinov, K. *J. Bacteriol.* **2009**, 191, 6273.
6. Vondenhoff, G. H. M.; Aerschot, A. V. *Eur. J. Med. Chem.* **2011**, 46, 5227.
7. Fang, P. f.; Jeong, S. J.; Mirando, A.; Chen, K.; Chen, X.; Kim, S.; Francklyn, C. S.; Guo, M. *Nat. Commun.* **2015**, 31, 6402.
8. Wang, S. F.; Yin, Y.; Qiao, F.; Wu, X.; Sha, S.; Zhang, L.; Zhu, H. L. *Bio. Med. Chem.* **2014**, 22, 2409.
9. Duan, Y. T.; Wang, Z. C.; Sang, Y. L.; Tao, X. X.; Zhu, H. L. *Curr Top Med Chem.* **2013**, 13, 3118.
10. Löfmark, S.; Edlund, C.; Nord, C. E. *Clin Infect Dis.* **2010**, 50, 16.
11. Freeman, C. D.; Klutman, N. E.; Lamp, K. C. *Drugs.* **1997**, 54, 679.

12. Luca, L.D. *Curr. Med. Chem.* **2006**, 13, 1.
13. Qin, Y. J.; Wang, P. F.; Makawana, J. A.; Wang, Z. C.; Wang, Z. N.; Gu, Y.; Jiang, A. Q.; Zhu, H. L. *Bioorg. Med. Chem.* **2014**, 24, 5279.
14. Wang, Z. C.; Duan, Y. T.; Qin, Y. J.; Wang, P. F.; Luo, Y.; Wen, Q.; Yang, Y. A.; Sun, J.; Hu, Y.; Sang, Y. L. Zhu, H. L. *Eur. J. Med. Chem.* **2013**, 65, 456.
15. Zhang, X.; Sangani, C. B.; Jia, L. X.; Gong, P. X.; Wang, F.; Wang, J. F.; Zhu, H. L.; *RSC Adv.* **2014**, 4, 54217.
16. Duan, Y. T.; Wang, Z. C.; Sang, Y. L.; Tao, X. X.; Teraiya, S. B.; Wang, P. F.; Wen, Q.; Zhou, X. J.; Ding, L.; Yang, Y. H.; Zhu, H. L.; *Eur. J. Med. Chem.* **2014**, 76, 387.
17. Li, J. R.; Li, D. D.; Wang, R. R.; Sun, J.; Dong, J. J.; Du, Q. R.; Fang, F.; Zhang, W. M.; Zhu, H. L.; *Eur. J. Med. Chem.* **2014**, 75, 438.
18. Erickson, J. A.; Jalaie, M.; Robertson, D. H.; Lewis, R. A.; Vieth, M. J. *J. Med. Chem.* **2004**, 47, 45.
19. Mao, W. J.; Lv, P. C.; Shi, L.; Li, H. Q.; Zhu, H. L.; *Bio. Med. Chem.* **2009**, 17, 7531.
20. Guizzunti, G.; Brady, T. P.; Malhotra, V.; Theodorakis, E. A.; *J. Am. Chem. Soc.* **2006**, 128, 4190.
21. Wang, S. F.; Yin, Y.; Qiao, F.; Wu, X.; Sha, S.; Zhang, L.; Zhu, H. L.; *Bio. Med. Chem.* **2014**, 22, 2409.
22. Sun, J.; Lv, P. C.; Guo, F. J.; Wang, X. Y.; Han, X.; Zhang, Y.; Sheng, G. H.; Qian, S. S.; Zhu, H. L. *Eur. J. Med. Chem.* **2014**, 81, 420.
23. Ghose, A. K.; Viswanadhan, V. N.; Wendoloski, J. J. *J. Phys. Chem. A.* **1998**, 102, 3762.
24. Discovery Studio 3.5 Guide, Accelrys Inc., San Diego, <http://www.accelrys.com>.
25. Lipinski, C. A.; Lombardo, F.; Dominy, B. W.; Feeney, P. J. *Adv. Drug Deliv. Rev.* **2001**, 46, 3.
26. Bruker Analytical X-ray Systems, SHELXTL-NT Versions 5.10 and 6.10 (**1999** and **2000**).

27. Wang, P. F.; Qiu, H. Y.; Ma, J. T.; Yan, X. Q.; Gong, H. B.; Wang, Z. C.; Zhu, H. L. *RSC Adv.* **2015**, *5*, 24997
28. The Clinical and Laboratory Standards Institute (formerly the National Committee for Clinical Laboratory Standards). Guideline M7–A6: Methods for dilution antimicrobial susceptibility tests for bacteria that grow aerobically. <http://www.ncccls.org>.
29. Hevener, K. E.; Mehboob, S.; Su, P. C.; Truong, K.; Boci, T.; Deng, J. P.; Ghassemi, M.; Cook, J. L.; Johnson, M. E. *J. Med. Chem.* **2012**, *55*, 268.
30. Xiao, Z. P.; Ma, T. W.; Liao, M. L.; Feng, Y. T.; Peng, X. C.; Li, J. L. Li, Z. P.; Wu, Y.; Luo, Q.; Deng, Y.; Liang, X.; Zhu, H. L. *Eur. J. Med. Chem.* **2011**, *46*, 4904.

Figure Captions

Table 1. Structures of compounds **5a-5w**.

Table 2. Crystal structure data for compound **5j**.

Table 3. Antibacterial activities of synthetic compounds.

Table 4. Inhibitory effects of the synthetic compounds against *S.aureus* tyrosyl-tRNA.

Table 5. Molecular parameters of synthetic compounds.

Fig. 1. The CDOCKER_INTERACTION_ENERGY (kcal/mol) obtained from the docking study of all synthesized compounds by the CDOCKER protocol (Discovery Studio 3.5, Accelrys, Co. Ltd).

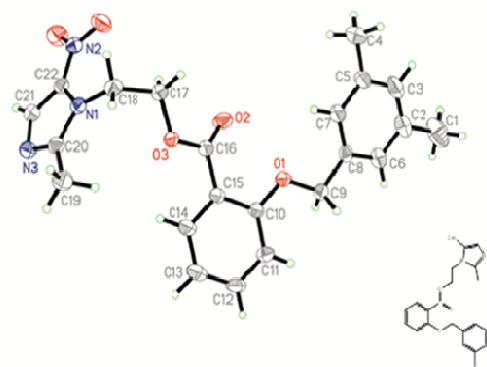
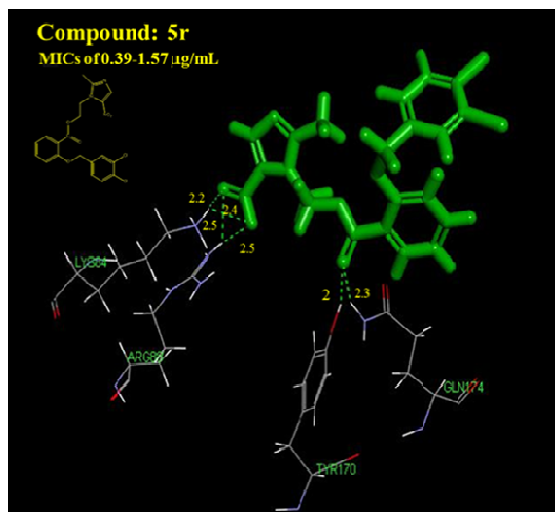
Fig. 2. Crystal structure diagram of compound **5j**.

Fig. 3. Molecular docking modeling of compound **5r** with *S. aureus* Tyrosyl tRNA synthetase: or clarity, only interacting residues are displayed.

Scheme 1. The synthetic routes of compounds **5a-5w**. Reagents and conditions:

(a) Et₃N, CH₂Cl₂, 0 °C, 6 h; (b) K₂CO₃, Me₂CO, 60 °C, 6~8 h; (c) NaOH, EtOH, 60 °C, 6 h, pH 1~3; (d) K₂CO₃, DMF, 110 °C, 20~24 h.

Graphical abstract

**Compound 5j**